SUPPORTING INFORMATION

for

Rapid Prototyping of Carbon-Based Chemiresistive Gas Sensors on Paper

Katherine A. Mirica, Joseph M. Azzarelli, Jonathan G. Weis, Jan M. Schnorr,

and Timothy M. Swager*

Department of Chemistry, Massachusetts Institute of Technology

77 Massachusetts Ave., Cambridge, MA 02139

* Corresponding author: Timothy M. Swager (tswager@mit.edu)

MATERIALS AND METHODS

General Materials and Methods. All chemicals and reagents were purchased from Sigma-Aldrich (Atlanta, GA) and used without further purification, unless noted otherwise. SWCNTs (purified ≥ 95% as SWCNT) were kindly provided by Nano-C, Inc. (Westwood, MA). MWCNTs (> 95 % carbon, outer diameter = 6–9 nm, average length = 5 μm, number of walls = 3–6) were purchased from Sigma-Aldrich (Atlanta, GA). Graphite Powder (natural, microcrystal grade, average particle size of 2-15 microns, 99.9995% [metal basis]) and Octafluoronaphthalene (CAS 313-72-4), 97% were purchased from Alfa Aesar (Ward Hill, MA). 2-(2-Hydroxy-1,1,1,3,3,3-hexafluoropropyl)-1-naphthol (CAS 2092-87-7), 97% was purchased from either SynQuest (Alachua, FL) or Santa Cruz Biotechnology (Santa Cruz, CA). Weighing Paper (Cat. No. 12578-165)—the substrate for the fabrication of sensors by mechanical abrasion— was purchased from VWR International (West Chester, PA). NH_3 (1% in N_2) and NO_2 (1% in air) were custom-ordered from Airgas.

Evaporation of Gold on Paper. Au electrodes (120 nm thickness) were deposited on the surface of paper through a stainless steel shadow mask (purchased from Stencils Unlimited, Lake Oswego, OR, http://www.stencilsunlimited.com/) using Thermal Evaporator (Angstrom Engineering, Kitchener, Ontario, Canada) under pressure of $1–4 \times 10^{-5}$ Torr and a rate of evaporation of 1–2 Å/s.

Ball Milling. Selective sensing materials were generated by solvent-free ball milling of carbon (e.g., SWCNTs) with commercial small molecule "selectors" using an oscillating mixer mill

(MM400, Retsch GmbH, Haan, Germany) within a stainless steel milling vial (5 mL) equipped with a single stainless steel ball (7 mm diameter). Unless otherwise indicated, a typical experiment involved filling the milling vial with carbon powder (e.g., SWCNTs) and selector (total mass of powder = 150 mg) and ball milling the mixture for 5 min at 30 Hz.

Fabrication of PENCILs. PENCILs were fabricated by loading powdered material into a mold, such as a pressing die set with 6-mm internal diameter (Across International, acrossinternational.com, Item # SDS6), or a pressing die set with 13-mm internal diameter (Sigma-Aldrich), or a custom-build die set with 2-mm internal diameter, and compressing the powder by applying a constant pressure of 10 MPa for 1 min using a Hydraulic Press (Carver, Model # 3912 or Across International Item # MP24A).

Fabrication of Sensors by DRAFT. Sensing materials were deposited on the surface of paper between gold electrodes by manual abrasion of the PENCIL. This process involved holding the 13-mm diameter pellet with a double gloved hand between the index finger and the thumb and manually rubbing the pellet on the surface of paper between the gold electrodes at a rate of ~ 10 mm/s with an applied force of ~ 1–5 N (estimated by abrading the pellet on the surface of paper using an analytical balance) several times to obtain the desired resistance of devices (typically ~10–50 kΩ). Precise control over the rate of deposition or the applied force was not necessary; we obtained good reproducibility in sensing response between devices examined in this study. Caution: Dust from carbon nanotubes and selectors may be harmful upon inhalation. To prevent potential inhalation of dust particles generated by the abrasion of PENCIL on paper, fabrication

of devices was carried out in a fume hood or on a benchtop while wearing a respirator face mask and safety glasses.

Sensing Measurements. The array of devices was mounted onto a 25 mm x 75 mm x 1 mm glass slide using a double-sided Scotch tape. The array was then inserted into a 2 x 30 pin edge connector (DigiKey), which made electrical contacts with each of the gold electrodes within the array. The edge connector was then connected to the potentiostat via a breadboard (DigiKey). For sensing measurements, the devices were enclosed within a custom-made gas-tight Teflon chamber containing an inlet and outlet port for gas flow. The inlet port was connected to a gas delivery system, and the outlet port was connected to an exhaust vent. Measurements of conductance were performed under a constant applied voltage of 0.1 V using PalmSense EmStat-MUX equipped with a 16-channel multiplexer (Palm Instruments BV, The Netherlands, http://www.palmsens.com/). Data acquisition was done using PSTrace 2.4 software provided by Palm Instruments. Matlab (R2011a, Mathworks) and Microsoft Excel were used to perform baseline correction, calculate relative sensing responses, and perform principal component analysis. Because some sensors showed partially reversible response toward certain analytes, where the magnitude of the sensing response from the first exposure to the analyte is significantly larger than the response from subsequent exposures, the sensing response of all sensors resulting from the first exposure to all analytes was excluded from calculating the average sensing response and the standard deviation.

Dilution of Gases. Delivery of controlled concentration of gases (NH_3 and NO_2) to devices were performed using Smart-Trak Series 100 (Sierra Instruments, Monterey, CA) gas mixing system at total flow rates of 1 L/min. NH_3 was diluted with N_2, and NO_2 was diluted with air.

Dilution of Vapors. Delivery of controlled concentrations of vapors to devices was carried out using Precision Gas Standards Generator Model 491M-B (Kin-Tek Laboratories, La Marque, TX). All vapors were diluted with N_2 at total flow rates of 0.25–0.50 L/min.

Microscopy. Scanning electron microscopy (SEM) was carried out using a JEOL JSM-6060 or JEOL JSM-6700F field emission SEM (FESEM) with energy-dispersive X-ray spectroscopy (EDX). Typical accelerating voltages were 1.5-5.0 kV.

Raman Spectroscopy. Raman spectra of solid composites of S^1 with various forms of nC were measured on a Horiba LabRAM HR Raman Spectrometer using excitation wavelength of 633 nm. Additional spectra were obtained for SWCNT/S^1 composites using excitation wavelengths of 532 nm and 784 nm. The spectra were collected with the following parameters in place: filter = none; hole = 1000 μm; slit = 100 μm; grating = 600; objective = 10x. In real-time-display mode, the spectral signal at 0 cm^{-1} was zeroed prior to acquisition. The spectrum was collected from 200 cm^{-1} to 3000 cm^{-1} with an integration time of 5 s averaged 100 times.

Measurements of Hardness of PENCILs. Ball-milled blends were compressed into pellets with thickness of ~1 mm using a hydraulic press. Measurements of mechanical hardness were carried out using Hysitron TriboIndenter equipped with a Berkovitch tip using quasi-static

indentation with typical applied loads ranging between 2–10 mN and depth of indentation ranging between 0.5 and 5 μm.

Measurements of Resistivity. Measurements of bulk conductance of compressed blends were carried out using an osmium four-point probe (Signatone, Part number: SP4-50-045-OFS) with a tip radius of 0.127 mm, space between tips of 1.27 mm, and spring pressure of 45 grams. Bulk conductance σ (S/cm) of samples was calculated using Eq. 1. In this equation, V (V) is the voltage, I (A) is the current, w (cm) is the thickness of a circular sample composite, C (unitless) is the geometry correction factor that accounts for a finite diameter of a circular sample composite, and F (unitless) is the thickness correction factor that accounts for a finite thickness of a circular sample composite.[1, 2]

$$\sigma = \mathrm{I}/(V \times w \times C \times \mathrm{F}) \quad (1)$$

Figure S1. Raman Spectroscopy of PENCILs (excitation wavelength = 632.7 nm) based on different mass ratios of S^1 with graphite, SWCNTs, and MWCNTs.

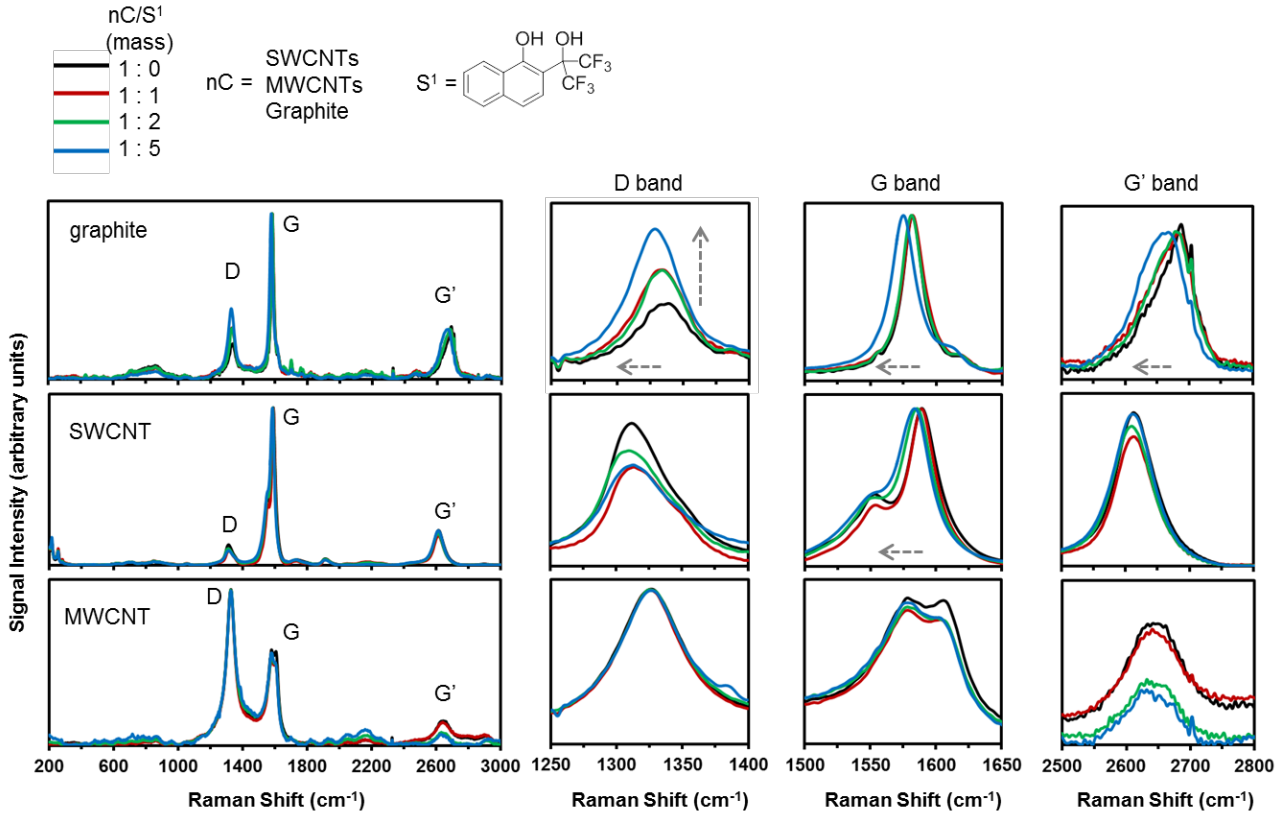

Figure S2. Raman Spectroscopy of SWCNT/S[1] composites at different excitation wavelengths.

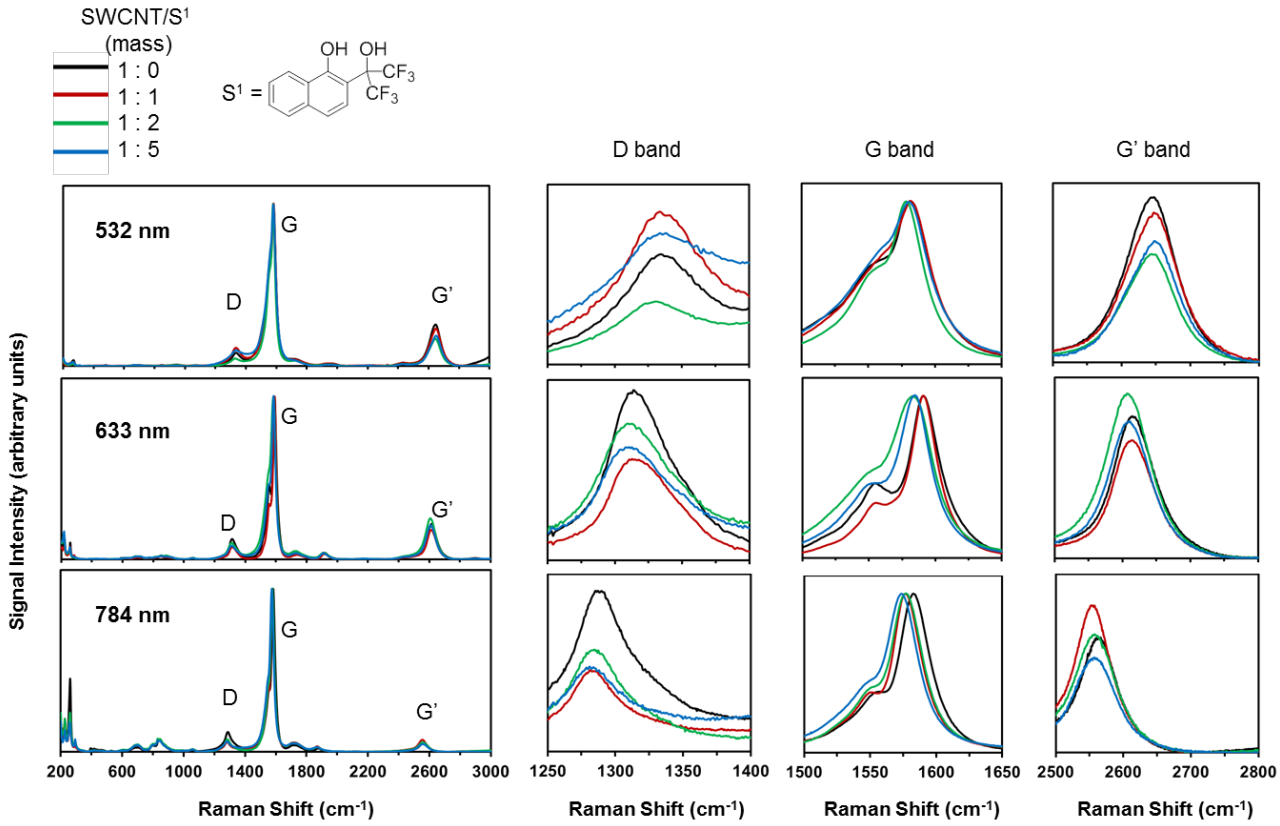

Figure S3. X-Ray survey scans of nC/S[1]composites.

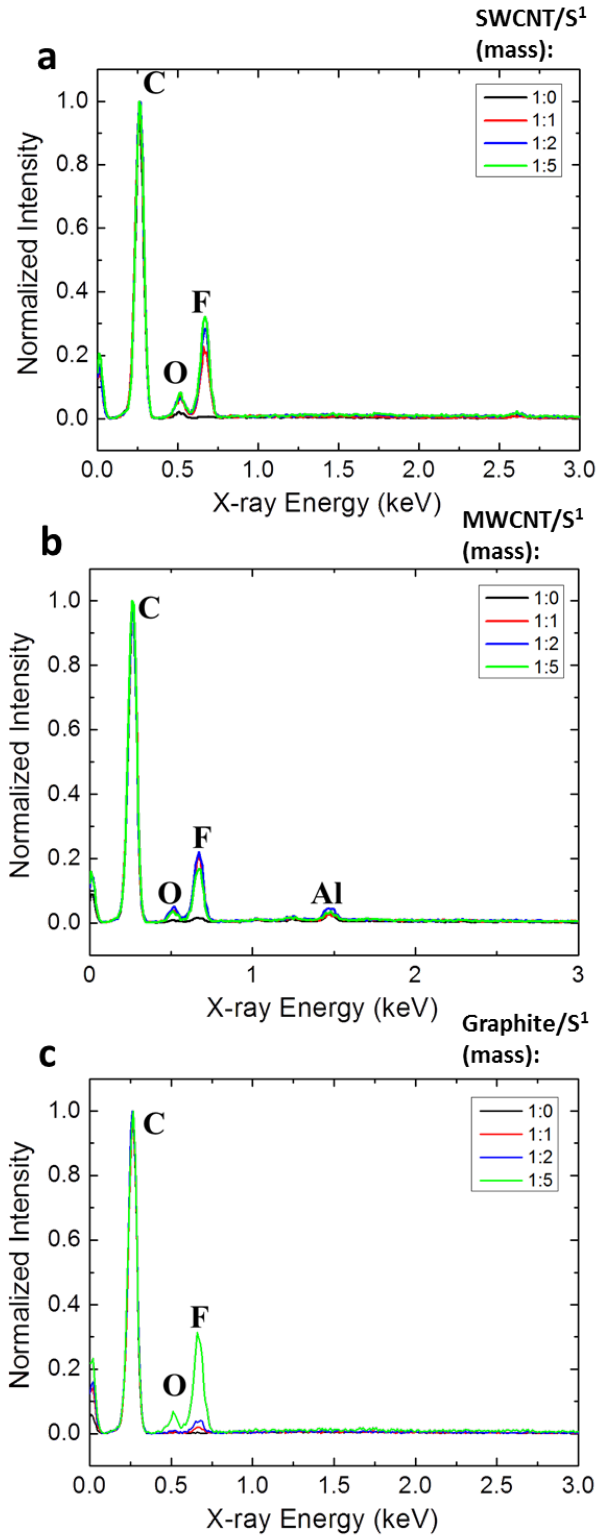

Figure S4. EDX of SWCNT/S[1] composites.

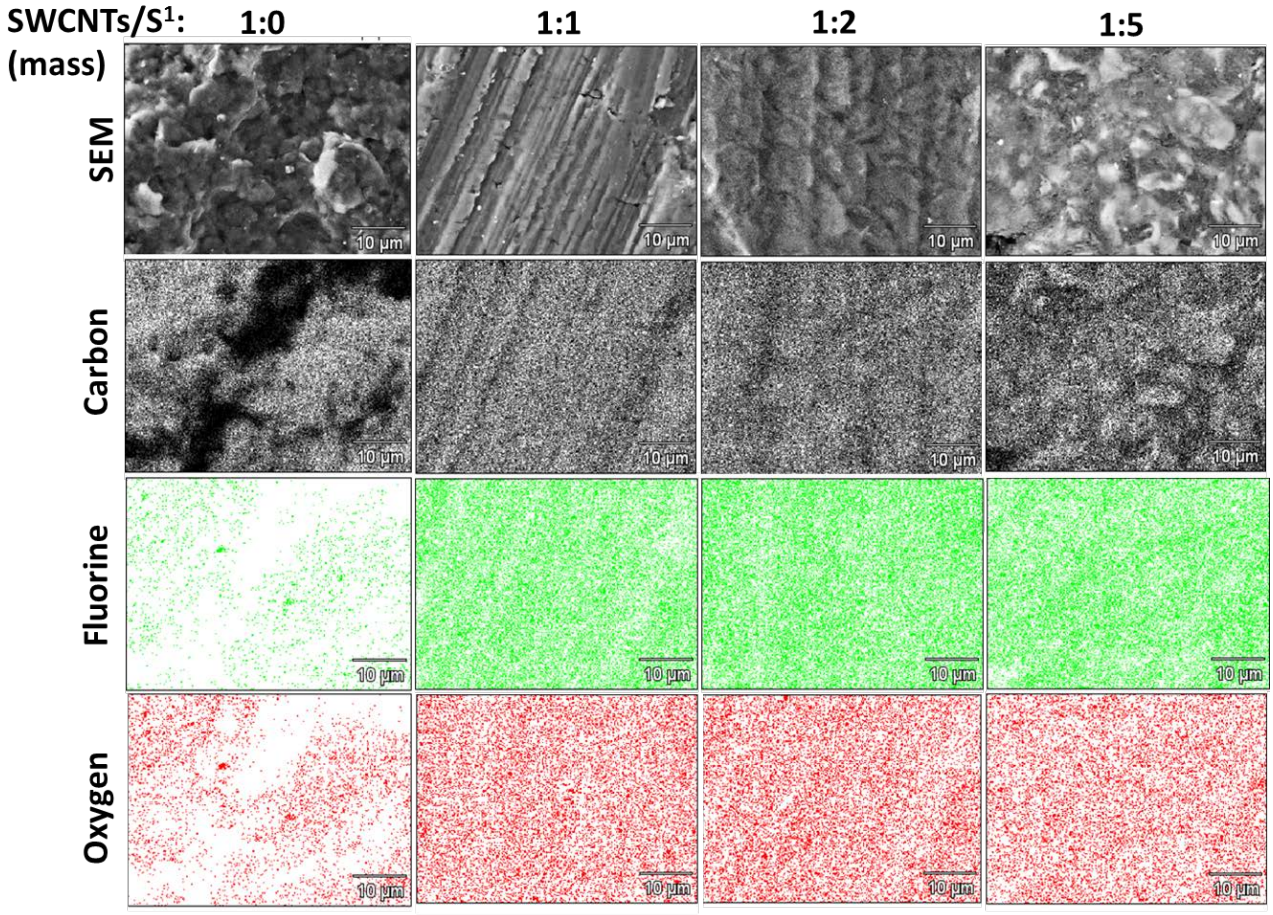

Figure S5. EDX of MWCNT/S[1] composites.

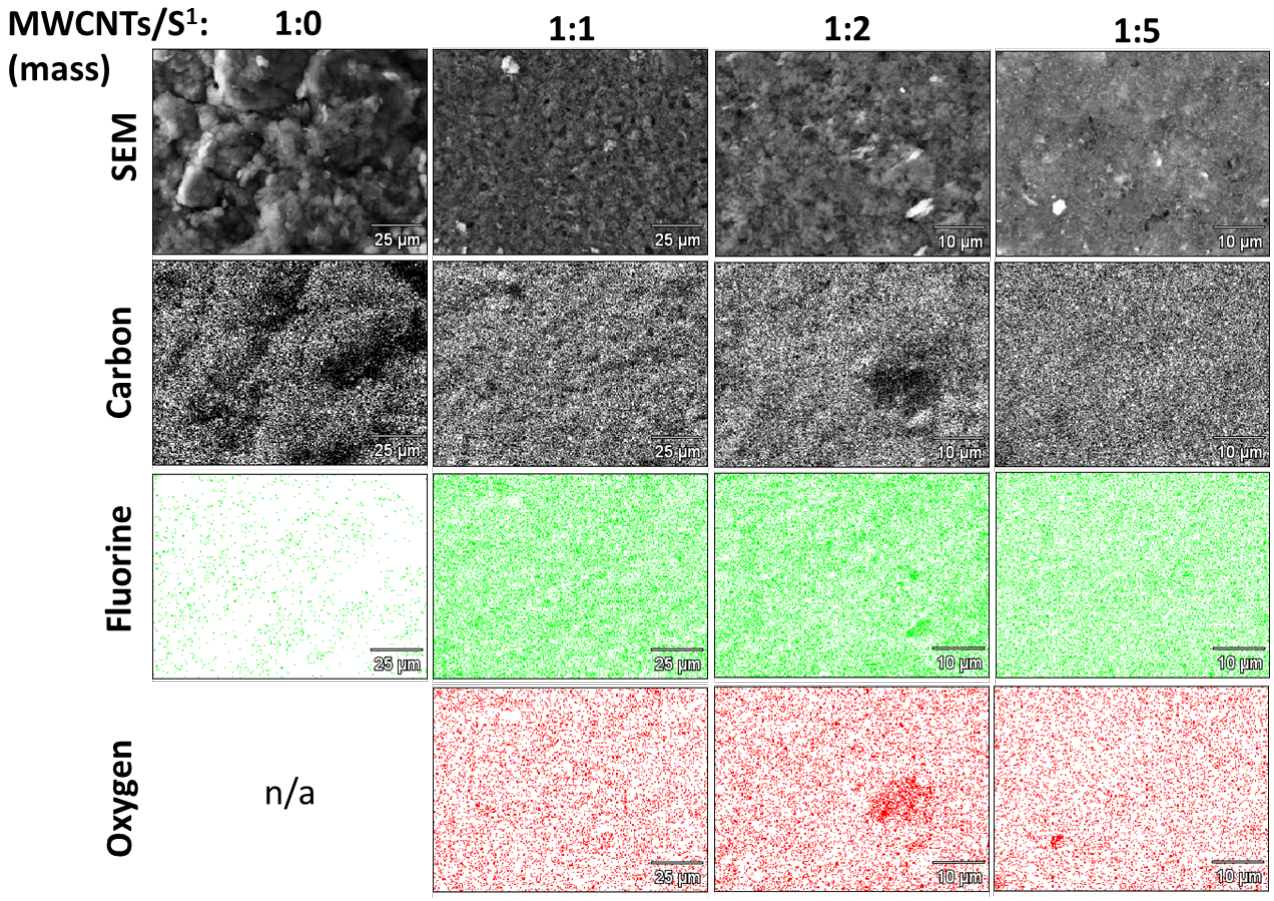

Figure S6. EDX of Graphite/S[1] composites.

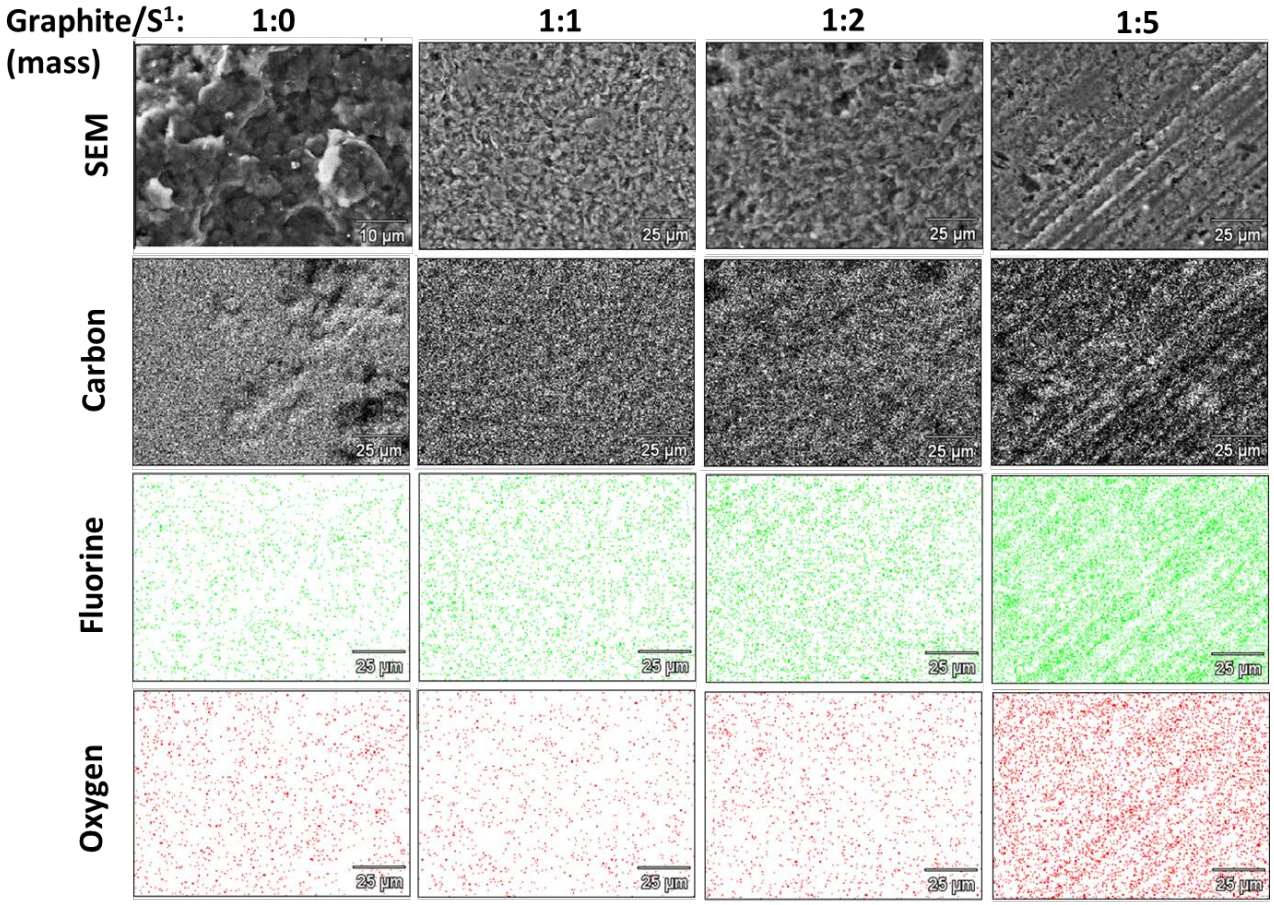

Figure S7. Photograph of selected sensors from the SWCNT-based array. Each sensor is drawn in triplicate on the surface of a paper chip between gold electrodes. Typical resistance range of sensors is 10 – 50 kΩ. The photograph shows two paper chips mounted on the surface of a glass slide using double sided tape.

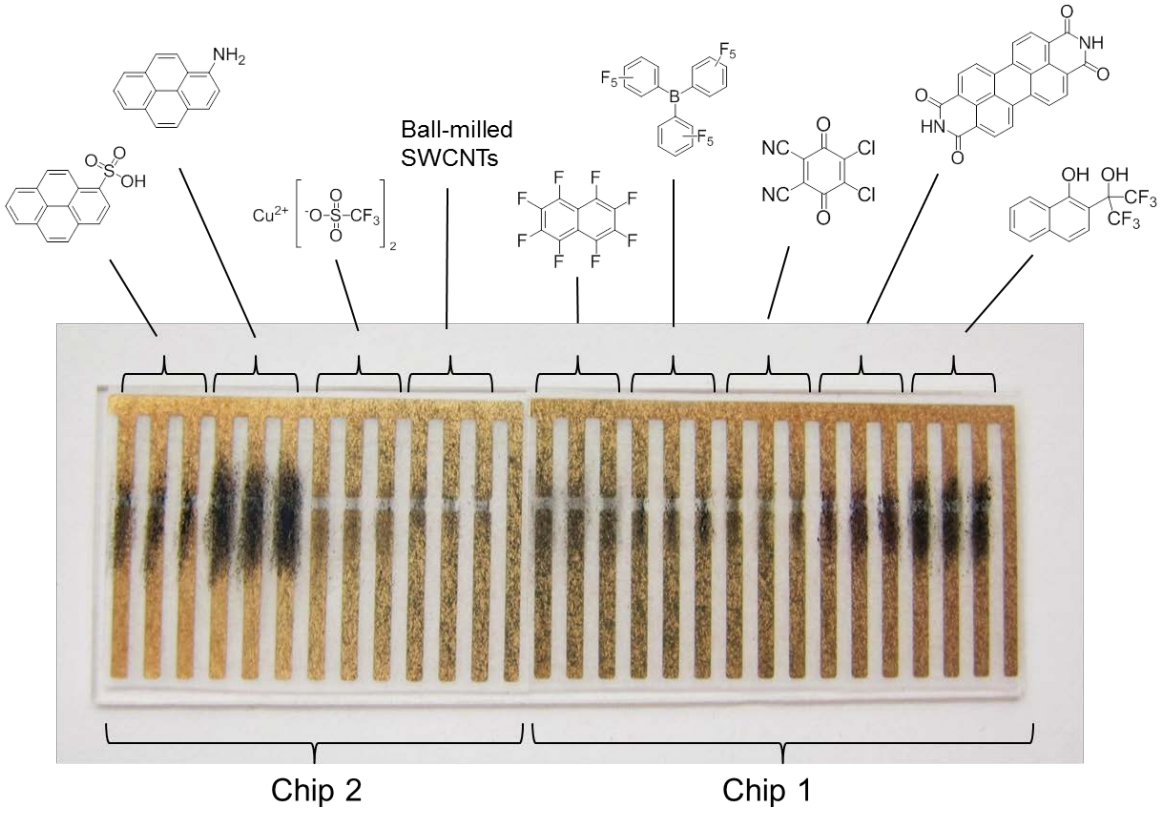

Figure S8. Sensing response ($-\Delta G/G_0$, %) with time of SWCNT-based array towards various analytes. No baseline correction. Each type of sensor was examined in triplicate. Multiple sensing responses for each type of sensor are overlayed to show reproducibility.

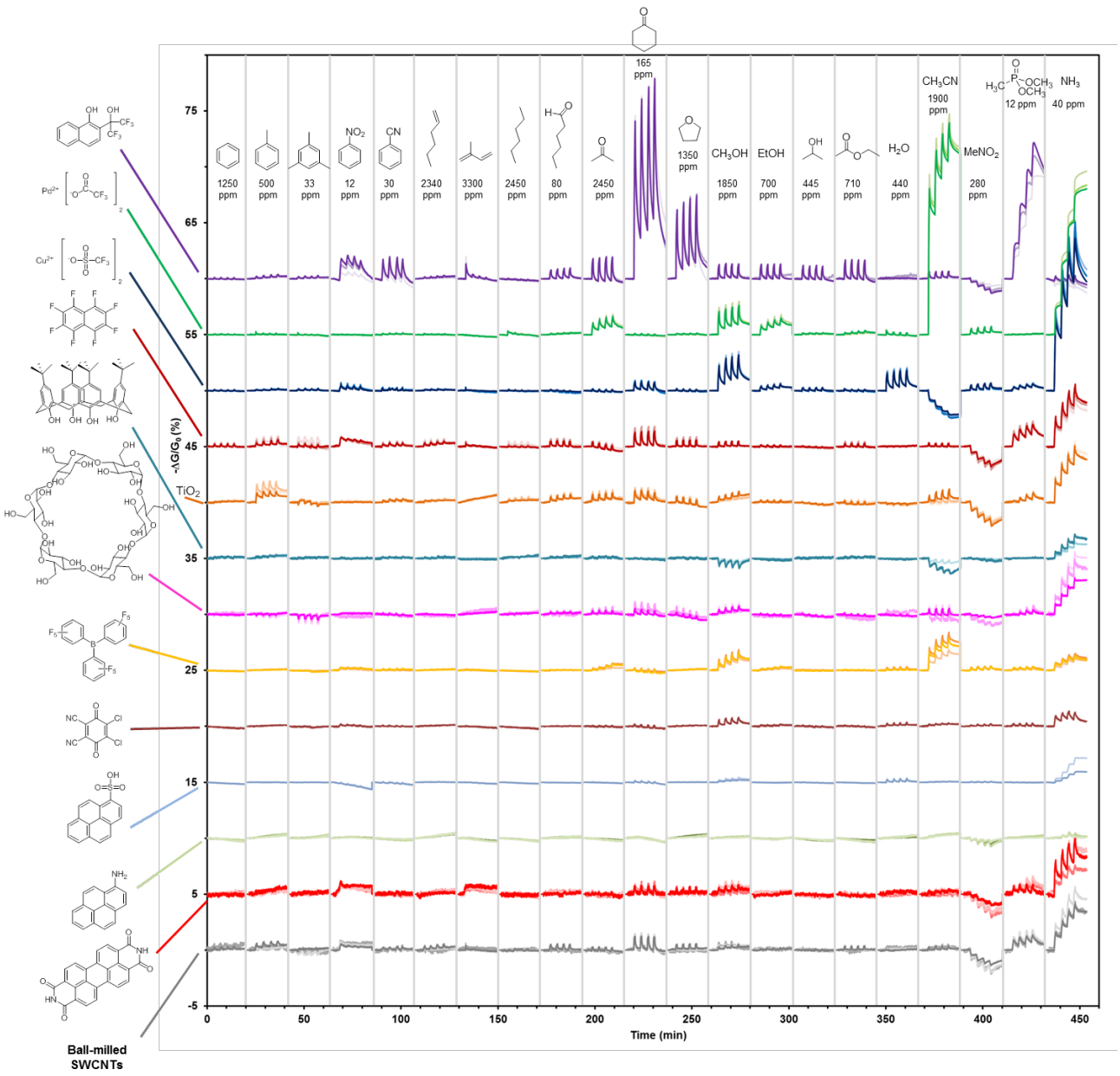

Figure S9. Sensing response ($-\Delta G/G_0$, %) with time of SWCNT-based array towards various analytes. Linear baseline correction was applied to all sensing responses. Each type of sensor was examined in triplicate. Multiple sensing responses for each type of sensor are overlayed to show reproducibility.

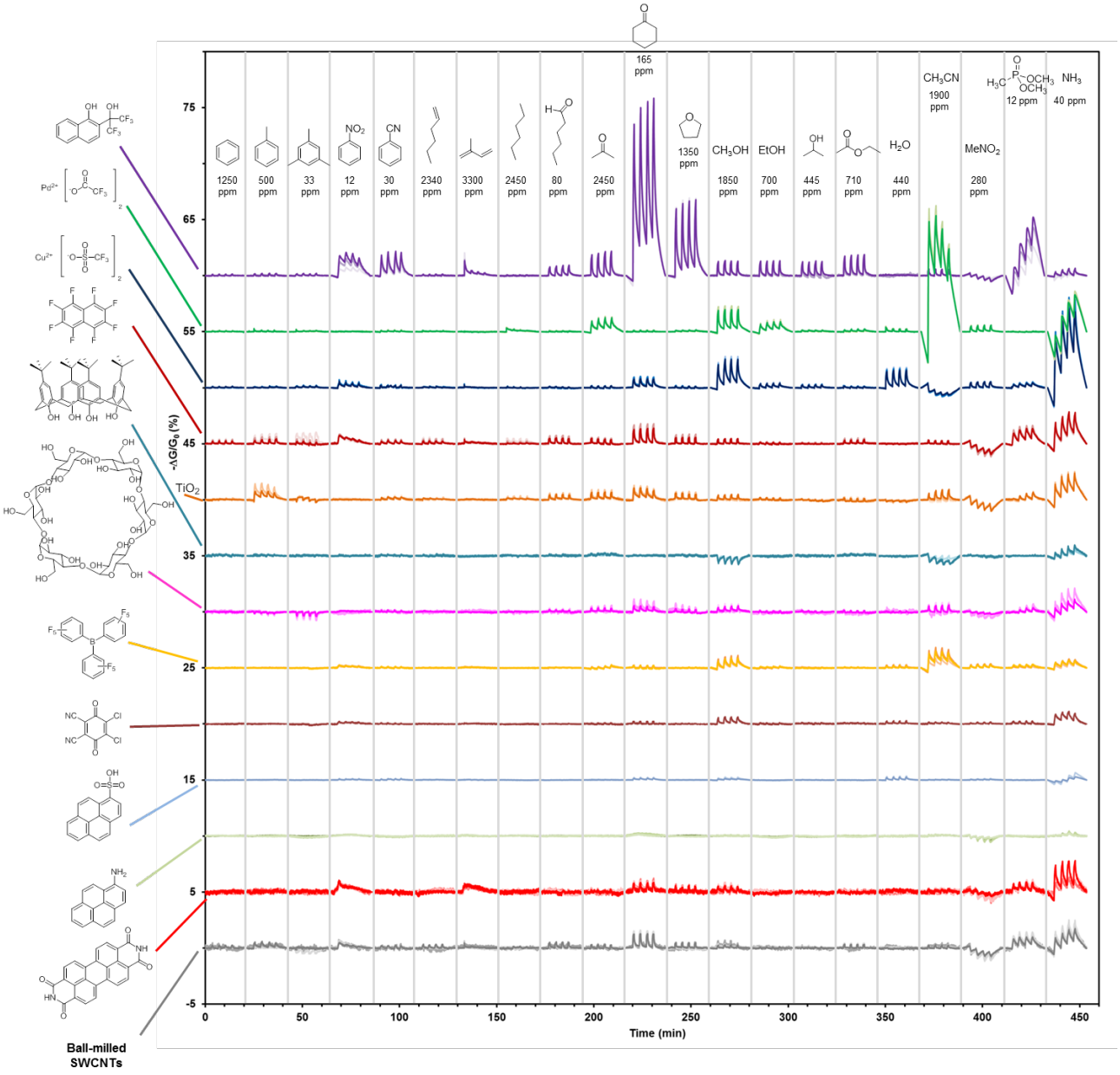

Figure S10. Sensing response ($-\Delta G/G_0$, %) with time of graphite-based array towards various analytes. No baseline correction was applied to the sensing responses. Each type of sensor was examined in triplicate. Multiple sensing responses for each type of sensor are overlayed to show reproducibility.

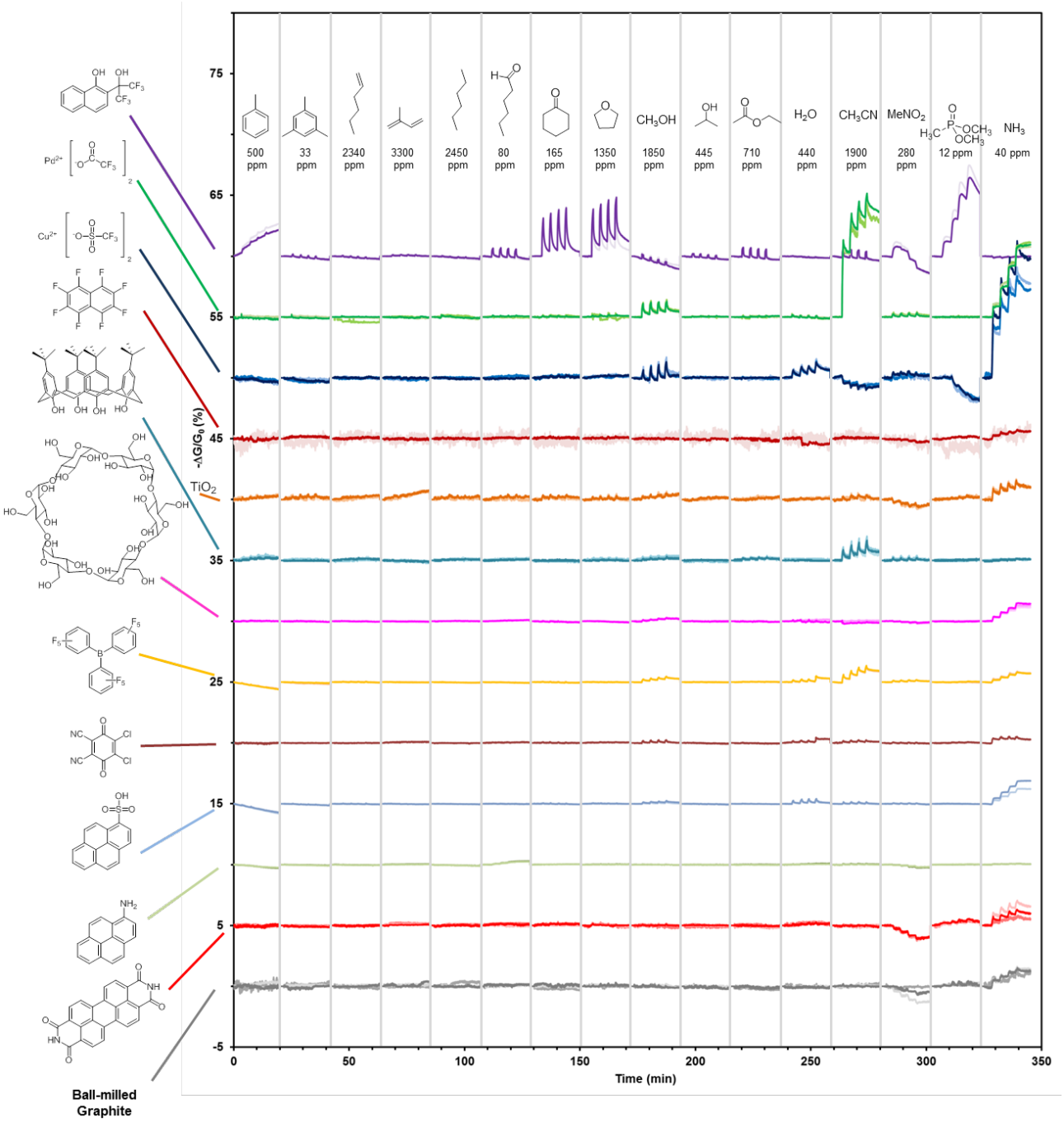

Figure S11. Sensing response ($-\Delta G/G_0$, %) with time of graphite-based array towards various analytes. Linear baseline correction was applied to all sensing responses. Each type of sensor was examined in triplicate. Multiple sensing responses for each type of sensor are overlayed to show reproducibility.

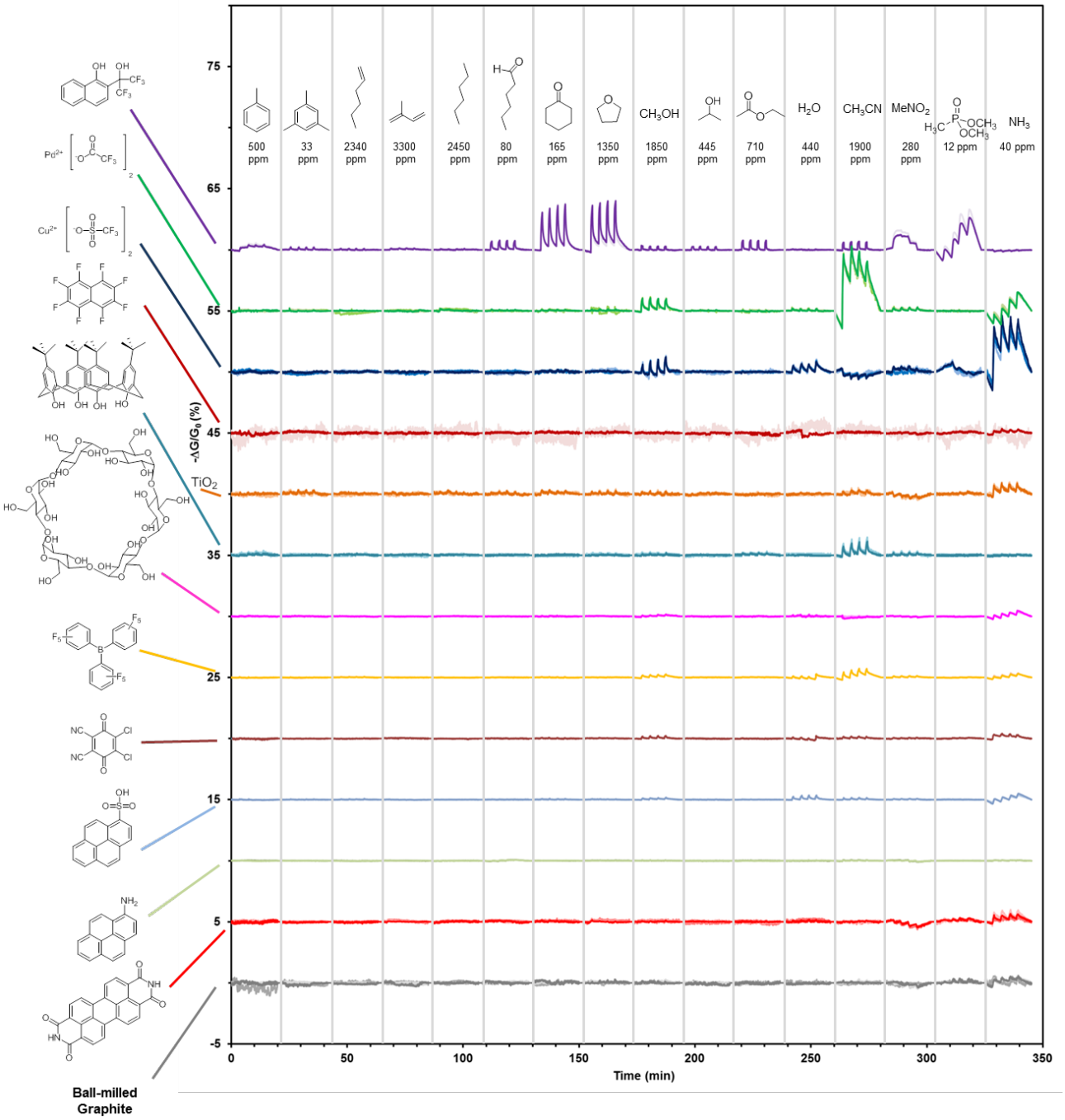

Figure S12. Sensing response of a cross-reactive array fabricated by mechanical abrasion of ball milled and compressed graphite and composites of graphite with selectors S^1–S^4 with (1:4 nC/S by mass) on the surface of weighing paper. Change in conductance (represented as $-\Delta G/G_0$, %) resulting from exposure of the array to eight vapors (at ~ 1 % equilibrium vapor pressure, specific concentrations as shown) and NH_3 gas (40 ppm). Each bar represents the average response of three sensors exposed to each analyte in triplicate. Vertical error bars represent the standard deviation from the average.

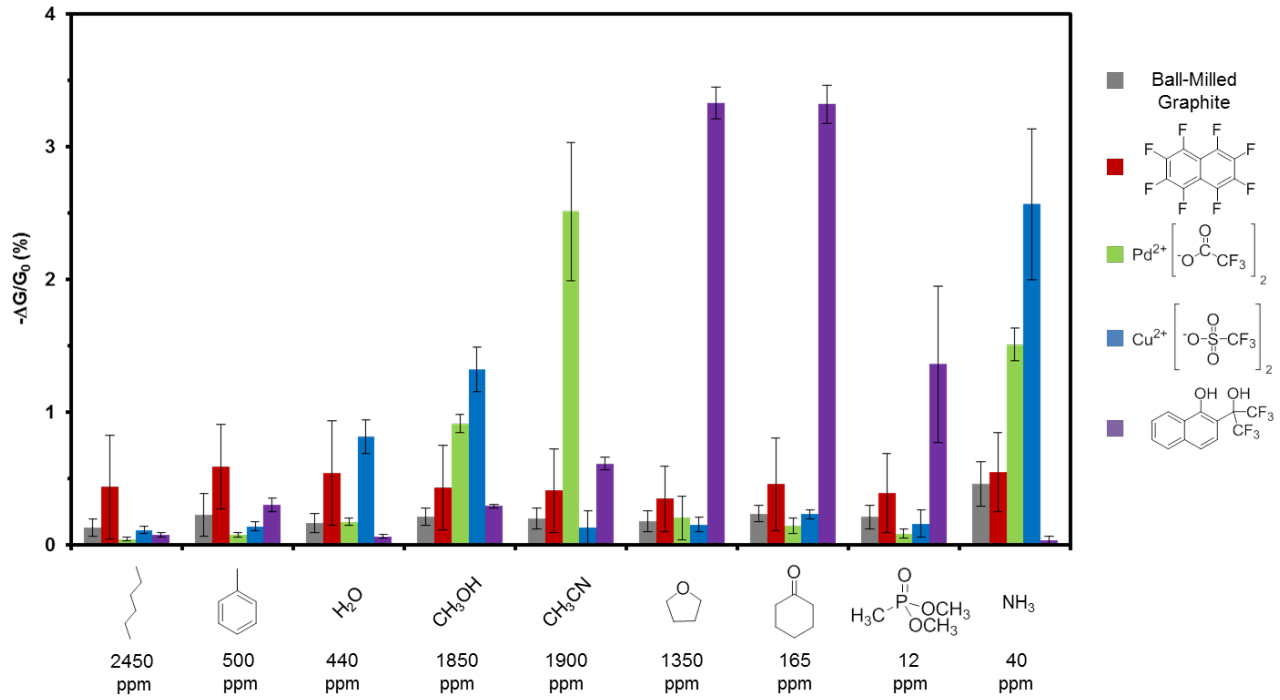

Figure S13. Quantitative comparison of sensing response ($-\Delta G/G_0$, %) toward water (a), ammonia (b), acetonitrile (c), and cyclohexanone (d) of sensors fabricated on the surface of weighing paper by mechanical abrasion of PENCILs comprising compressed blends of graphite and SWCNTs with S^1- S^4 (1:4) by mass. Vertical error bars represent standard deviation from the mean based on three exposures of three sensors to each of the analytes.

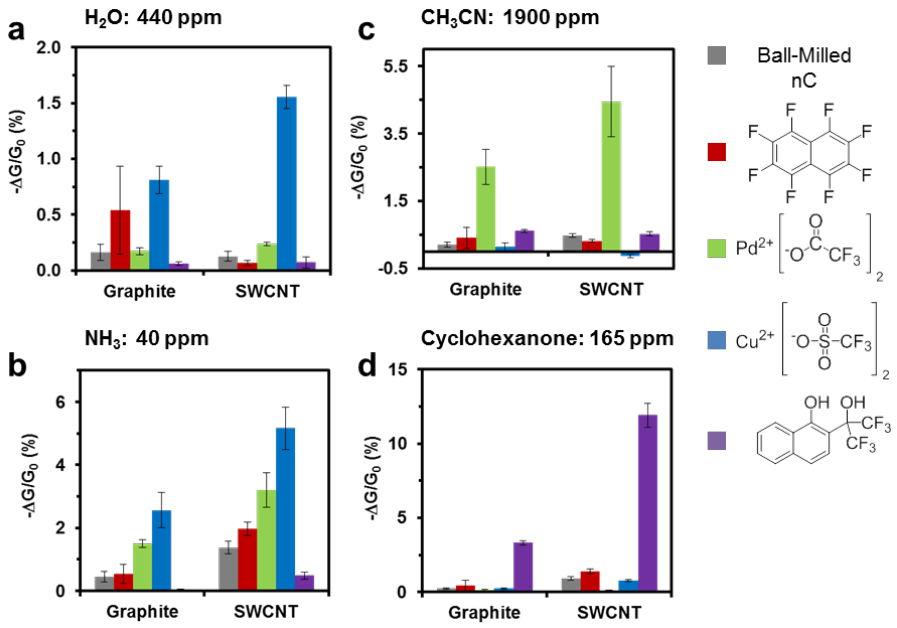

Figure S14. Principal component analysis (PCA) of SWCNT-based array toward ten selected analytes with 3D and 2D projections of principal components.

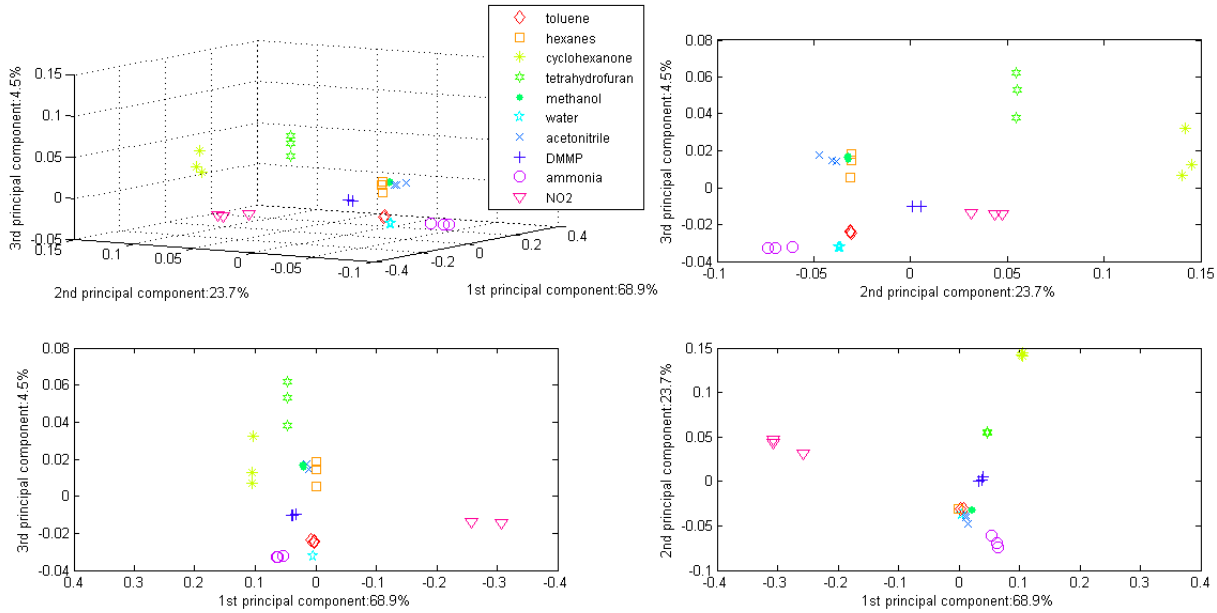

Figure S15A. Principal component analysis (PCA) of the sensing response of the graphite-based array toward nine selected analytes with 3D and 2D projections of principal components.

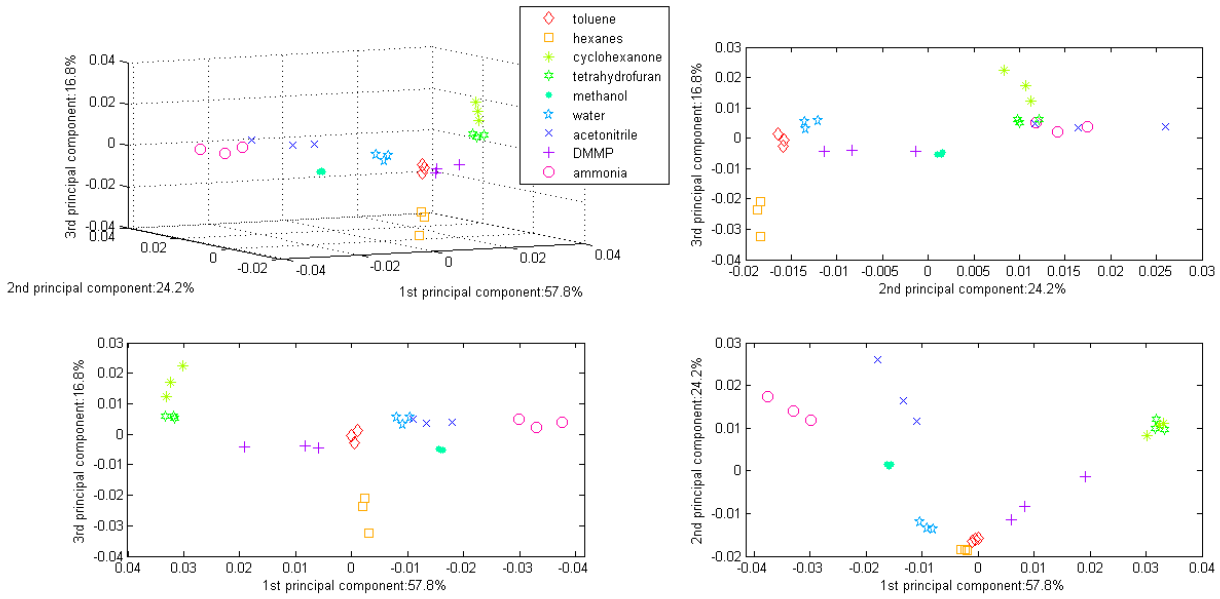

Figure S15B. Principal component analysis (PCA) of the response of SWCNT-based array toward nine selected analytes with 3D and 2D projections of principal components.

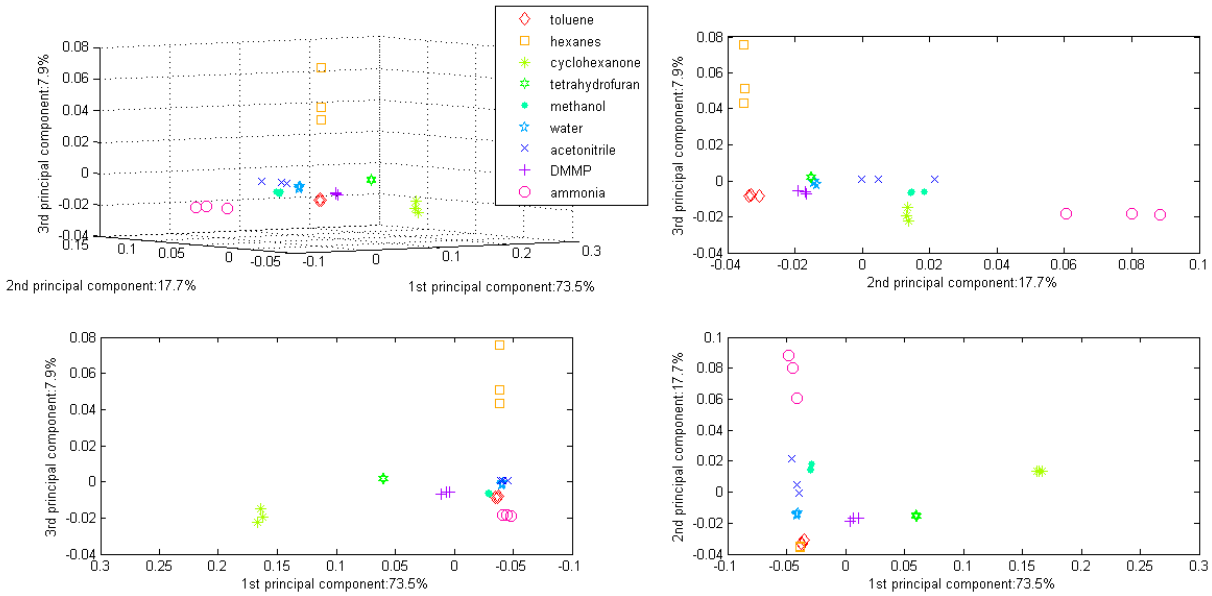

Figure S16. X-Ray survey scans of solid composites of a) SWCNTs/$Cu(OSO_2CF_3)_2$ and b) SWCNTs/$Pd(OCOCF_3)_2$ both 4:1 by mass.

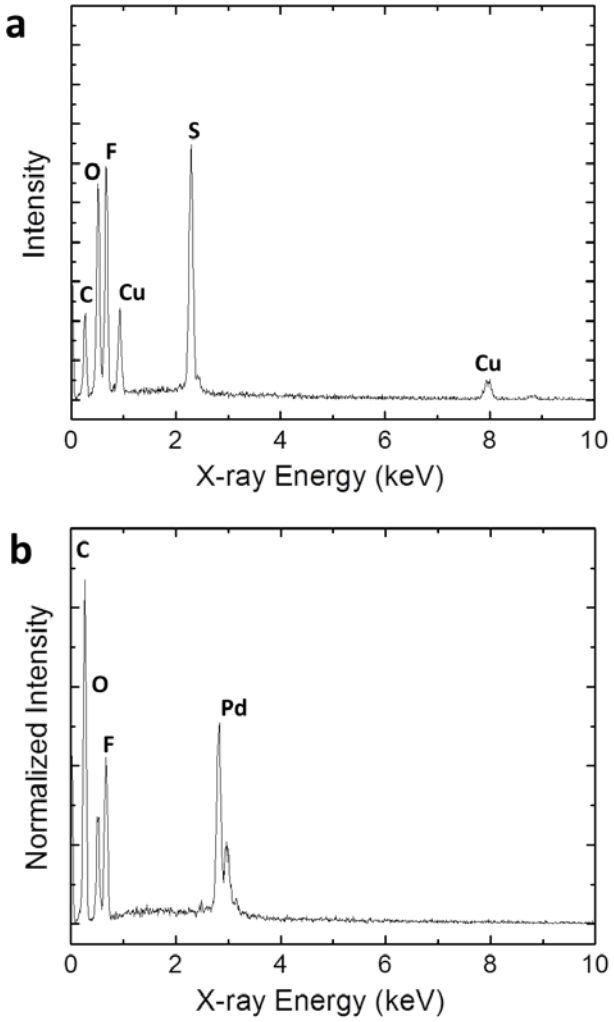

Figure S17. EDX of solid composites of SWCNTs/$Cu(OSO_2CF_3)_2$ and SWCNTs/$Pd(OCOCF_3)_2$ both 4:1 by mass.

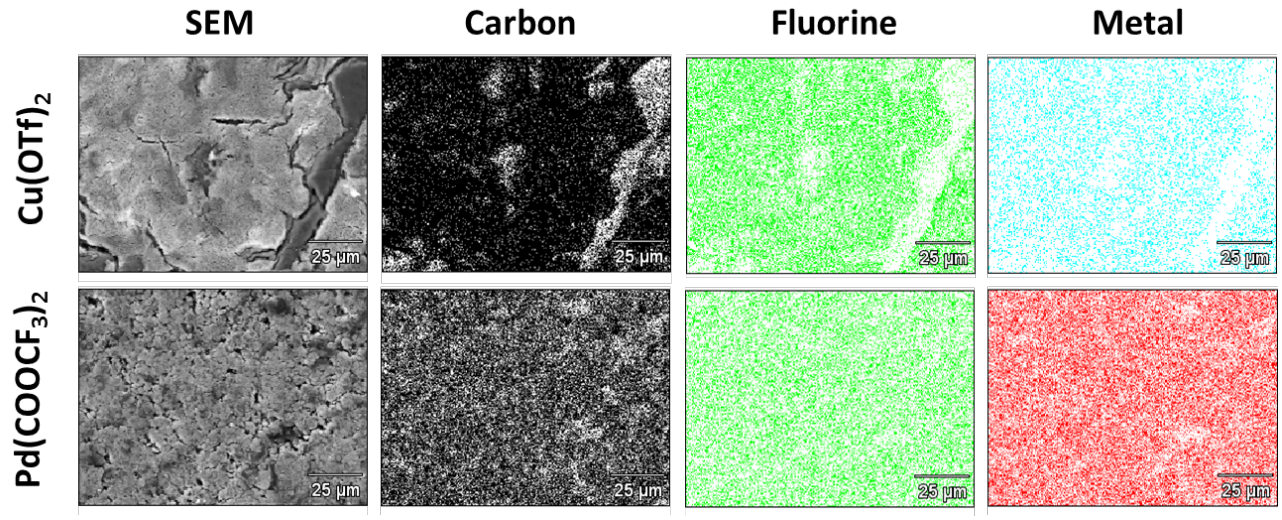

Figure S18. SEM images of solid composites of a) SWCNTs/$Cu(OSO_2CF_3)_2$ and b) SWCNTs/$Pd(OCOCF_3)_2$ both 4:1 by mass.

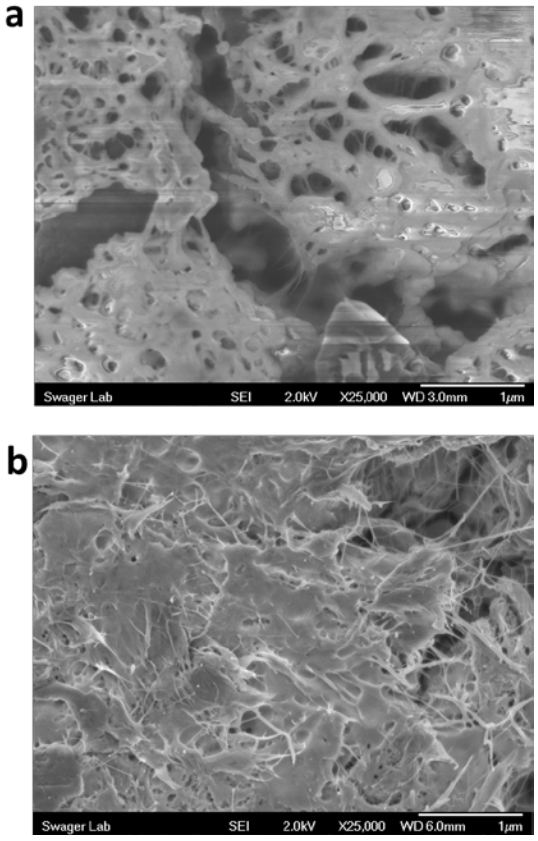

Table S1. Bulk conductivity σ of nC/S[1] composites.

	σ (S/cm)	σ (S/cm)	σ (S/cm)
nC/S[1]	nC = SWCNTs	nC = MWCNTs	nC = Graphite
1 : 0	256 ± 5	14.9 ± 0.2	884 ± 28
1 : 1	56 ± 2	13.1 ± 0.1	82 ± 3
1 : 2	25 ± 1	11.3 ± 0.1	21.9 ± 0.3
1 : 5	2.3 ± 0.1	3.1 ± 0.1	1.4 ± 0.3

Table S2. Hardness (*H*) of nC/S[1] composites.

	H (MPa)	*H* (MPa)
nC/S[1]	nC = SWCNTs	nC = Graphite
1 : 0	118 ± 53	478 ± 262
1 : 1	160 ± 62	21 ± 7
1 : 2	59 ± 34	98 ± 57
1 : 5	7 ± 4	176 ± 72

Table S3. Bulk conductivity σ of 1:4 nC/S composites used for rapid prototyping of sensing arrays.

	σ (S/cm)	σ (S/cm)
S (Scheme 1)	nC = SWCNTs	nC = Graphite
1	2.2 ± 0.2	3.13 ± 0.03
2	17 ± 1	35 ± 2
3	8 ± 7	0.61 ± 0.07
4	48 ± 7	11 ± 2
5	43 ± 8	4.0 ± 0.1
6	0.32 ± 0.02	0.91 ± 0.04
7	12.5 ± 0.2	3.0 ± 0.2
8	8.0 ± 0.3	11.5 ± 0.2
9	19 ± 3	18.8 ± 0.5
10	28 ± 1	3.2 ± 0.1
11	0.20 ± 0.01	40 ± 3
12	30 ± 3	8.4 ± 0.1

References:

1. Collins, WR, Schmois, E and Swager, TM (2011) Graphene oxide as an electrophile for carbon nucleophiles. *Chem Comm* **47:** 8790-8792.

2. Smits, FM (1958) Measurement of sheet resistivities with the four-point probe. *Bell Syst Tech J* **May:** 711-718.